Supplemental Figures

Probe	Target organism	Sequence	Hybridization Buffer % Formamide	Reference	Fluorophores: CLASI-FISH Set 1	Fluorophores: CLASI-FISH Set 2	Fluorophores: FISH
Eub_338 I	Eubacterial	gctgcctcccgtaggagt	20	Amann et. al 1990	Cy5	Cy5	Cy5*
Eub_338 III	Eubacterial	gctgccacccgtaggtgt	20	Amann et. al 1990	Cy5	Cy5	Cy5*
Alph_968	Alphaproteobacteria	ggtaaggttctgcgcgtt	20	Glöckner et. al 1998	Atto 532	Dy-610	Cy3
Verruco_193	Verrucomicrobia	cgccattacaagctttagta	20	Collins et. al 2012	Texas Red - X	Atto-532	Cy5
Gamma_42a	Gammaproteobacteria	gccttcccacatcgttt	20	Manz et. al 1992	DY-610	Texas Red-X	Atto-488
Leis_194	Leisingera	accgactagcatgctagccg	30	This study	Rhodamine Red-X	DY-490	* Applied to seriel section
Rueg_66	Ruegeria	gctcaccccgaaaggcgcgc	30	This study	DY-490	Rhodamine Red-X	

Supplemental Table 1: FISH probes and experimental designs used in study.

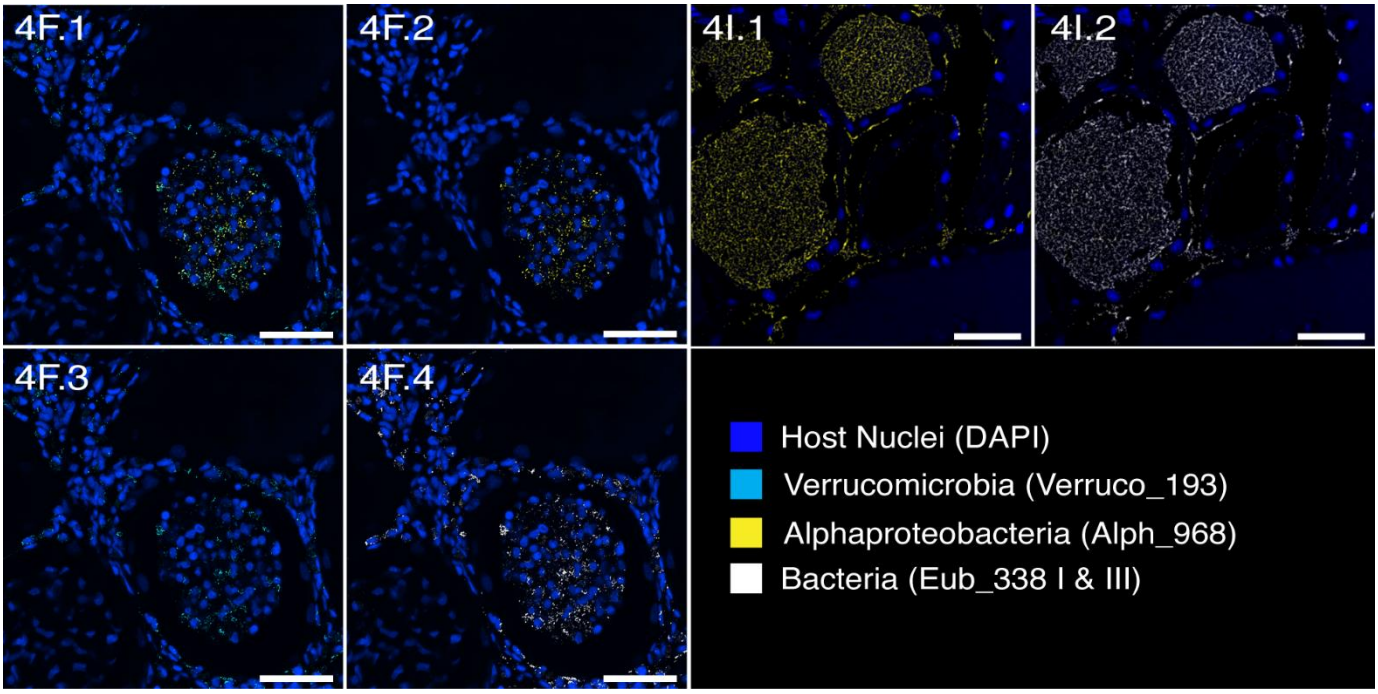

Supplemental Figure 1: Split image channels and eubacteria probe positive controls for FISH images in Fig. 4. (4F.1) Image in Fig. 4F. (4F.2) DAPI and Alphaproteobacteria channels. (4F.3) DAPI and Verrucomicrobia channels. (4F.4) DAPI and eubacteria channels. Eubacteria channel shows bacterial distribution nearly identical to that in 4F.1 (4I.1) Image in Fig. 4I. (4I.2) DAPI and eubacteria channels. Bacterial distribution in the eubacteria channel is nearly identical to that in 4I.1 Scale bars: 4F.1-4 = 75 µm; 4I.1&2 = 50 µm

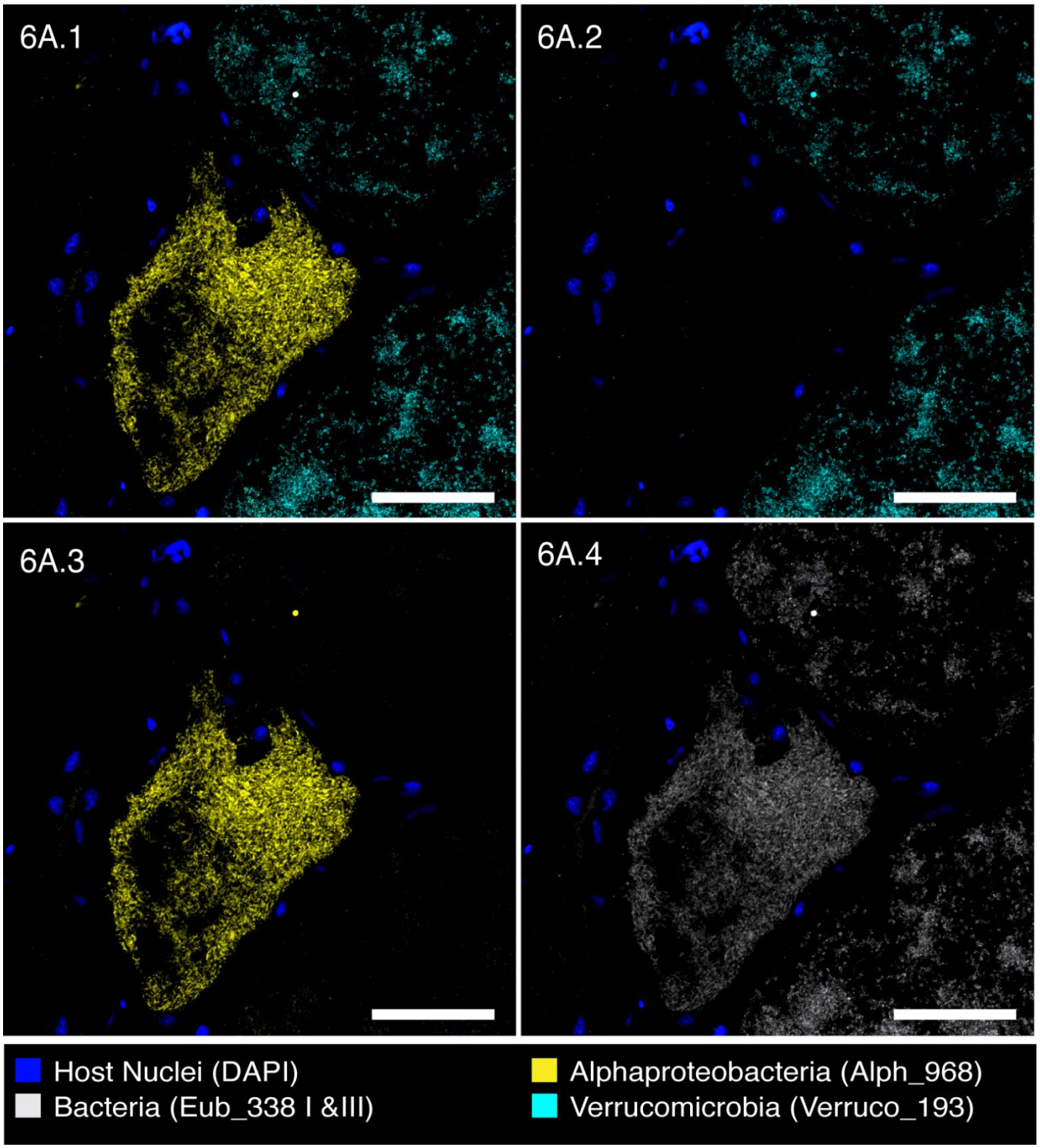

Supplemental Figure 2: Split image channels and eubacteria probe positive controls for FISH images in Fig. 6. (6A.1) Image in Fig. 6A. (6A.2) DAPI and Verrucomicrobia channels. (6A.3) DAPI and Alphaproteobacteria channels. (6A.4) DAPI and eubacteria channels. Eubacteria channel shows bacterial distribution nearly identical to that in 6A.1 Scale bars: 75 μm

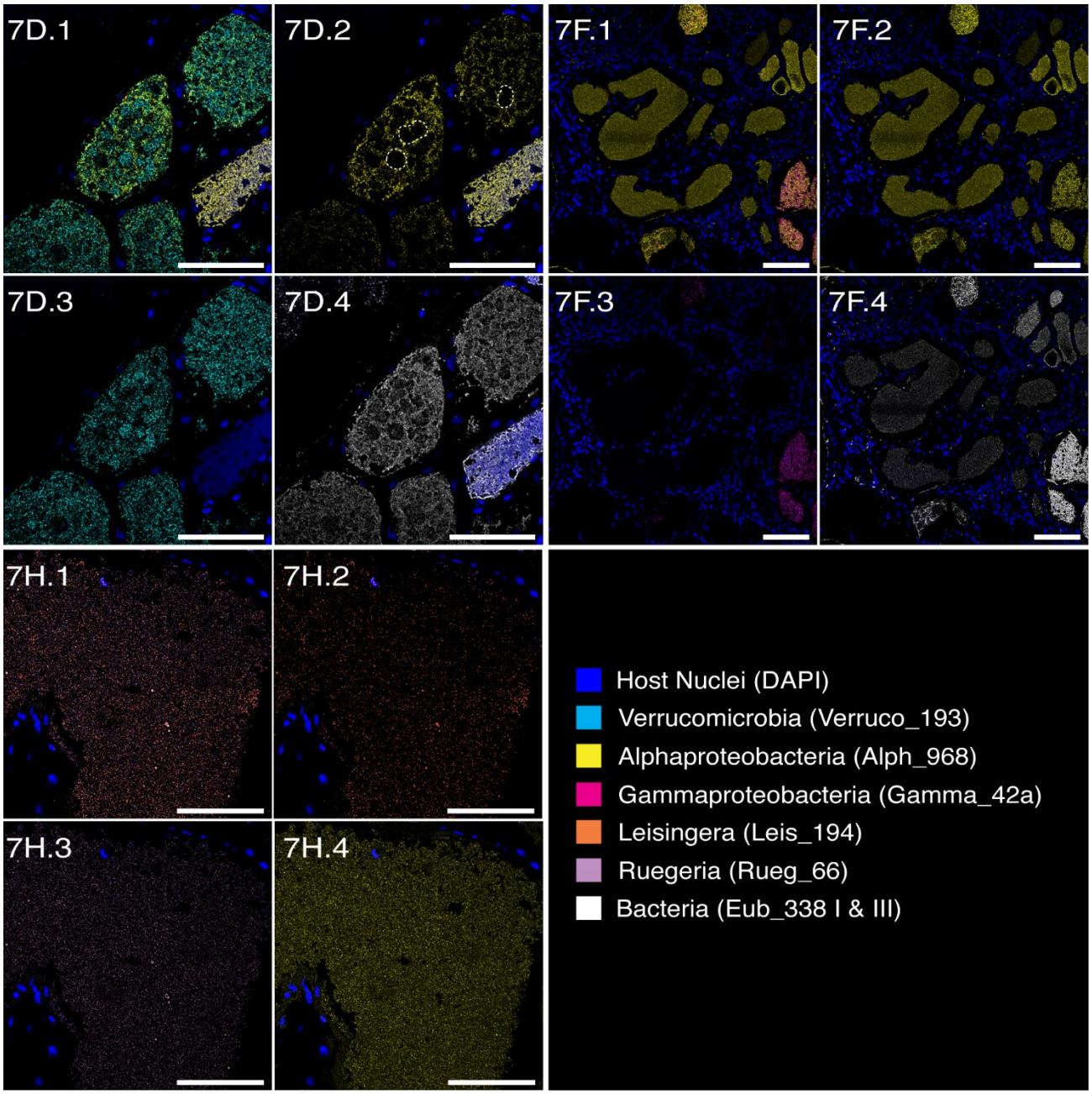

Supplemental Figure 3: Split image channels and higher taxonomic level probe positive controls for FISH images in Fig. 7. (7D.1) Image in Fig. 7D. (6D.2) DAPI and Alphaproteobacteria channels. (7D.3) DAPI and Verrucomicrobia channels. (7D.4) DAPI and eubacteria channels. Eubacteria channel shows bacterial distribution nearly identical to that in 7D.1 (7F.1) Image in Fig. 7F. (7F.2) DAPI and Alphaproteobacteria channels. (7F.3) DAPI and Gammaproteobacteria channels. (7F.4) DAPI and eubacteria channels. Bacterial distribution in the eubacteria channel is nearly identical to that in 7F.1 (7H.1) Image in Fig. 7H. (7H.2) DAPI and Leisingera channels. (7H.3) DAPI and Ruegeria channels. (7H.4) DAPI and Alphaproteobacteria channels. Alphaproteobacteria channel shows bacterial distribution nearly identical to that in 7H.1 Scale bars: 7D.1-4 = 50 µm; 7F.1-4 = 100 µm 7H.1-4 = 50 µm

Supplemental Video 1: Three dimensional features of whole ANG. (0:00) 3D transparency projection of whole ANG captured on light sheet microscope seen in Fig. 2A. (0:03) 3D maximum intensity projection. (0:07) Tubules within the dorsal 1/3 of ANG are disorganized and cross over medial plane. (0:11) Tubules within the middle of the ANG display bilateral symmetry on both sides of the medial plane (red plane). (0:17) Individually traced tubules of the whole ANG. (0:28) Traced tubules superimposed onto 3D transparency projection.

Supplemental Video 2: Tubule convergence underneath NG. (0:00) 3D volume projection of quadrant of ANG seen in Fig. 2F. (0:04) Inter-gland space highlighted in yellow. (0:13) The inter-gland space is lined with pores at which ANG tubules terminate. (0:18) Individually traced tubules converge at point underneath the NG. Sectioning into tissue illustrates tracing of ANG tubules. (0:31) Some converging tubules weave back and forth through imaging planes. (0:37) 3D maximum intensity projection of ANG quadrant, as seen in Fig. 2G.

Supplemental Video 3: The inter-gland space in 3D. (0:00) 3D volume projection of quadrant of ANG seen in Fig. 2F. Inter-gland space is highlighted in purple. (0:06) Segmenting into tissue to reveal inter-gland space between ANG and NG. (0:12) The inter-gland space is lined with pores at which ANG tubules terminate. (0:20) The inter-gland space is highlighted in purple; orientation and segmentation is as seen in Fig. 3C.

Supplemental Video 4: Visualizing Bacterial Deposition from ANG. Video showing small debris spinning in the inter-gland space between the NG (top left) and ANG. Peristaltic motion of ANG tubules appears to push tubule contents towards the inter-gland space.